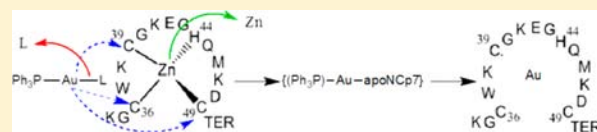


Gold(I)-Phosphine-N-Heterocycles: Biological Activity and Specific (Ligand) Interactions on the C-Terminal HIVNCp7 Zinc Finger

Camilla Abbehausen,[†] Erica J. Peterson,[‡] Raphael E. F. de Paiva,[†] Pedro P. Corbi,[†] André L. B. Formiga,[†] Yun Qu,^{‡,§} and Nicholas P. Farrell^{*,‡,§}[†]Institute of Chemistry, University of Campinas—UNICAMP, P.O. Box 6154, CEP 13083-970, Campinas, São Paulo, Brazil[‡]Goodwin Laboratory, Massey Cancer Center, Virginia Commonwealth University, 401 College Street, Richmond, Virginia 23298, United States[§]Department of Chemistry, Virginia Commonwealth University, 1001 W. Main Street, Richmond, Virginia 23284-2006, United States

Supporting Information

ABSTRACT: The syntheses and the characterization by chemical analysis, ¹H and ³¹P NMR spectroscopy, and mass spectrometry of a series of linear triphenylphosphine gold(I) complexes with substituted N-heterocycle ligands (L), [(PPh₃)Au(I)(L)]⁺, is reported. The reaction of [(PPh₃)Au(L)]⁺ (L = Cl⁻ or substituted N-heterocyclic pyridine) with the C-terminal (Cys₃His) finger of HIVNCp7 shows evidence by mass spectrometry (ESI-MS) and ³¹P NMR spectroscopy of a long-lived {(PPh₃)Au}-S-peptide species resulting from displacement of the chloride or pyridine ligand by zinc-bound cysteine with concomitant displacement of Zn²⁺. In contrast, reactions with the Cys₂His₂ finger-3 of the Sp1 transcription factor shows significantly reduced intensities of {(PPh₃)Au} adducts. The results suggest the possibility of systematic (electronic, steric) variations of “carrier” group PR₃ and “leaving” group L as well as the nature of the zinc finger in modulation of biological activity. The cytotoxicity, cell cycle signaling effects, and cellular accumulation of the series are also reported. All compounds display cytotoxicity in the micromolar range upon 96 h continuous exposure to human tumor cells. The results may have relevance for the reported inhibition of viral load in simian virus by the gold(I) drug auranofin.



INTRODUCTION

Gold-based complexes with biological activity represent a wide variety of chemotypes. The orally active antiarthritic drug auranofin inhibits tumor growth *in vitro*, motivating investigation of the chemical and biological properties of Au(I)-phosphine compounds.^{1–3} In blood, the thiosugar of auranofin is rapidly displaced by serum albumin residues, followed by phosphine displacement and formation of R₃P=O.² The rate of displacement of the phosphine ligand is determined by the basicity of the phosphine, but systematic studies of the influence of the “leaving group” (chloro, organothiols, etc.) on the activity are relatively sparse for N-donor ligands. In this article, we show the synthesis, characterization, cytotoxicity, and studies on zinc-finger interactions of a new series of [(PPh₃)Au(I)L]⁺ compounds (where L = Cl⁻ or substituted N-heterocyclic pyridine) capable of systematic modification on both ligands, Figure 1.

The inherently “soft” nature of Au(I) has long suggested thiol interactions as possible modes of action of these drugs.^{1,2} Notably, thioredoxin has been reviewed as a target^{1,4} as have cysteine proteases,⁵ and most recently even glutathione peroxidase and trypanothione reductase.^{6,7} Early studies on antiarthritic gold complexes suggested a plausible mode of action as inhibition of zinc fingers through metal ion displacement.^{8,9} Biophysical studies of a variety of Au(I) and Au(III) compounds on zinc fingers do indeed show rapid displacement of Zn(II) with formation of “gold fingers” where

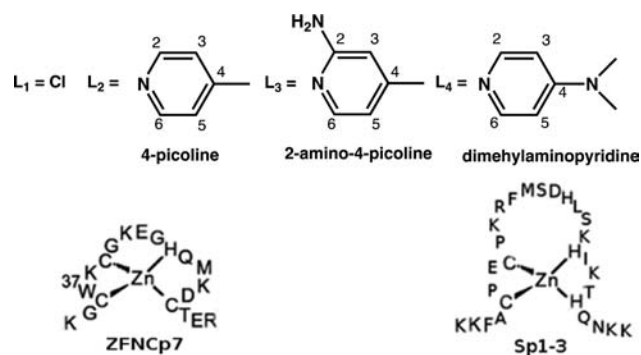


Figure 1. Structures of the [(PPh₃)AuL]⁺ series and the zinc finger peptides used in this study.

all ligands attached to the gold center are lost.^{10–13} An intrinsic issue in considering zinc fingers as targets is that of specificity. We therefore examined the interactions of the [(PPh₃)Au(L)]⁺ series with prototypical zinc finger peptides differing in the zinc coordination sphere: the Cys₂His₂ finger-3 of the Sp1 transcription factor and the Cys₃His C-terminal finger of HIVNCp7 nucleocapsid protein. The latter produces a long-lived [(PPh₃)Au]-peptide(S-donor) species upon reaction, the first observation of a Au(ligand)-zinc finger species. The

Received: June 17, 2013

Published: September 24, 2013

Table 1. ^1H , ^{13}C , and ^{31}P NMR; ESI-MS Spectrometry m/z Ions; and λ_{max} for the Studied Compounds^a

^1H δ (ppm) ^b multiplicity, integration	^{31}P δ (ppm) ^c	^{13}C δ (ppm) ^b	m/z	λ_{max} (nm)
Compound I				
7.42–7.58 (0.16) m, 15H (Ph)	30.8 (38.7)	127.91 (–0.78)	721 [(Ph ₃ P)Au(PPh ₃) ⁺	204 (199.5)
		128.81 (0.01)	476 [(Ph ₃ P=O)Au] ⁺	
		128.97 (0.02)	952 [Au(Ph ₃ P=O)] ₂ ⁺	
		131.64 (–5.76)		
		133.70 (–0.14)		
		133.88 (–0.22)		
Compound II				
8.69 (0.24), d, 2H	27.1 (–3.7)	21.83 (0.61)	721 [(Ph ₃ P)Au(PPh ₃) ⁺	201 (204)
2.47 (0.14), s, 3H		127.51 (2.68)	552 [(Ph ₃ P)Au(C ₆ H ₇ N)] ⁺	
		150.73 (0.97)	459 [(Ph ₃ P)Au] ⁺	
		153.73 (6.51)	476 [Au(Ph ₃ P=O)+H] ⁺	
			500 [Au(PPh ₃)(CH ₃ CN)] ⁺	
Compound III				
6.84 (0.52), s, 1H	28.2 (–2.6)	21.70 (0.48)	567 [(Ph ₃ P)Au(C ₆ H ₈ N ₂) ⁺	200 (199)
6.51 (0.05), br, 1H		113.68 (4.54)	721 [(Ph ₃ P)Au(PPh ₃) ⁺	
6.42 (2.19), d, 1H		115.24 (0.55)		
2.40 (0.07), s, 3H		153.05 (5.06)		
		158.59 (0.00)		
Compound IV				
8.33 (–0.10), d 2H	27.5 (–3.3)	39.22 (0.01)	581 [(Ph ₃ P)Au(C ₇ H ₁₀ N ₂) ⁺	200 (203, 256)
6.49 (0.30), d, 2H		107.44 (0.73)	721 [(Ph ₃ P)Au(PPh ₃) ⁺	
3.11 (0.64), s, 6H		148.78 (1.28)		
		155.28 (0.90)		

^aNumbers in parentheses indicate the difference between the gold(I) complex and the free ligand (L or PPh₃). ^bReferenced to TMS. ^cReferenced to CH₃PO₄.

reaction is zinc-finger specific and is not observed under similar conditions for the Cys₂His₂-based Sp1 transcription factor.

EXPERIMENTAL METHODS

Materials. All reagents used in this study were reagent grade and used without further purification. Aurochloric acid trihydrate, H[AuCl₄].3H₂O, was purchased from StremChem (Newburyport, MA). Triphenylphosphine (PPh₃) was purchased from Sigma Aldrich in 99% purity grade. 4-Picoline (L2, pic), 2-amine-4-picoline (L3), dimethylaminopyridine (L4, DMAP), and *N*-acetyl-L-cysteine (N-AcCys) were purchased from Sigma Aldrich. Apo-peptides were purchased by GenScript Corporation and have the following sequences: NCp7-F2 (KGCWKCKGKEGHQMKDCTER), monoisotopic mass 2224.47 Da; Sp1-F3 (KKFACPECP-KRFMSDHLKHIKTHQNKK), monoisotopic mass 3366.95 Da. The zinc finger peptides were prepared according to our published procedures (refs 12 and 33) and characterized with known samples by CD (Figure 5A,B), ^1H NMR and mass spectrometry. The other reagents used in this study are common.

Physical Measurements. For complex characterization, ^1H , ^{13}C , and ^{31}P NMR spectra were recorded on a Varian Mercury series 300 MHz NMR spectrometer using a 5 mm probe. ^1H and ^{13}C were referenced to trimethylsilane (TMS), and ^{31}P was referenced to trimethylphosphate (CH₃)₃PO₄. Samples were dissolved in deuterated chloroform (CDCl₃) with 99% deuterium content and 0.1% (v/v) TMS. Trimethylphosphate was added in 0.1% (v/v) amount for ^{31}P NMR acquisition. For gold compound–peptide studies, the stock solutions of the peptide, zinc acetate, and gold compounds were prepared in the same conditions described above using deuterated solvents D₂O and CD₃CN. pH adjustments were made using NaOD. The molar ratio was 1:1.3 (peptide/Zn²⁺) and 1:1.3 (ZF/Au⁺). ^{31}P NMR spectra were recorded on a Bruker Avance series 600 MHz NMR spectrometer using a 5 mm probe. ^{31}P was referenced to trimethylphosphate (CH₃)₃PO₄.

Electrospray ionization time-of-flight mass spectrometry (ESI-TOF-MS) evaluations were conducted on a Waters/Micromass QTOF-2

instrument operated in positive ion mode. Solutions were injected in 3:1 acetonitrile (ACN)/acetic acid mixture at a flow rate of 3 $\mu\text{L min}^{-1}$, using a source voltage of 2.34 kV and a cone voltage of 30 V. The source temperature was maintained at 85 °C throughout. Collision gas was introduced into the hexapole to aid in ion cooling. Elemental analysis was performed by Quantitative Technologies Inc., Whitehouse, NJ. UV–vis spectra were recorded with a JascoV550 UV–vis spectrophotometer (Easton, MD) equipped with a Jasco ETC 505T temperature controller and a VWR thermostat using a low headspace microcuvette with 10 mm path and 150 μL volume. Fluorescence experiments were conducted with a Cary Eclipse fluorescence spectrophotometer (Agilent Technologies, Santa Clara, CA) using a cuvette with 10 mm path and 3 mL volume. The temperature adjustment was made by a Peltier module and magnetic stirring. Inductive coupled plasma–mass spectrometry measurements were performed with a Varian ICP-MS. Potentiometric titrations were performed using the Metrohm Titrino Plus 848 automatic titrator, with a dosing buret of 10 000 steps and a glass electrode. The measurements were performed in the dynamic mode. Samples were prepared dissolving compounds I, II, and IV, 1 mmol L^{–1}, in CH₃CN/H₂O 5:1, with KCl 0.05 mol L^{–1}. KOH 3 mmol L^{–1} in CH₃CN/H₂O 5:1, with KCl 0.05 mol L^{–1}, was used as titrant. Potentiometric titration curves were analyzed with CurTiPot 3.6.1, to obtain the pK_a values.¹⁴

Synthesis of Chlorotriphenylphosphinegold(I) (I). [(Ph₃P)-AuCl] I was synthesized as previously described.¹⁵ In brief, tetrachloroauric acid trihydrate H[AuCl₄].3H₂O (1 mmol, 0.3938 g) was dissolved in a 1:1 ethanol/acetone (3 mL) mixture. Triphenylphosphine, PPh₃ (2 mmol, 0.5245 g) in chloroform (6 mL), was added to the solution of chloroauric acid with stirring. The yellow color of the solution disappeared and a white precipitate immediately formed. The solid was recovered by filtration, washed with ethanol/acetone and ethyl ether and dried in the desiccator. Yield: 78% (0.3859 g). Anal. Calcd (%) for C₁₈H₁₅ClPAu: C, 43.7; H, 3.06. Found (%): C, 43.9; H, 3.17.

Synthesis of [(Ph₃P)AuL]NO₃ (II–IV). A 0.3 mmol portion of I was dissolved in chloroform (3 mL) under stirring. A 0.3 mmol

portion of AgNO_3 dissolved in 2 mL of a 1:1 mixture of ethanol/acetone was added to the solution. AgCl precipitated immediately and was removed by filtration. Portions (0.3 mmol) of L2–4 were dissolved in 1 mL of chloroform and added to the activated gold-triphenylphosphine solution. The mixture was kept under stirring for 24 h followed by removal of the solvent under vacuum. The yellowish film was dissolved in acetone, and drops of ether were added precipitating the white solid. Solution was removed, and the solid was dried under vacuum. Principal characterizing data shown; full details in Table 1.

$[(\text{Ph}_3\text{P})\text{Au}(\text{C}_6\text{H}_7\text{N})]\text{NO}_3$ (II). Characterization data follow. White powder. Yield: 43% (80 mg). NMR δ (^1H) 7.42–7.58 (m, 17H); 8.69 (d, 2H); 2.47 (s, 3H). δ (^{31}P) 27.1 ppm; m/z 552 $[(\text{Ph}_3\text{P})\text{Au}(\text{C}_6\text{H}_7\text{N})]^+$. Anal. Calcd (%) for $\text{C}_{24}\text{H}_{22}\text{N}_2\text{O}_3\text{PAu}$: C, 46.9; H, 3.32; N, 4.31. Found (%): C, 46.9; H, 3.61; N, 4.56.

$[(\text{Ph}_3\text{P})\text{Au}(\text{C}_6\text{H}_8\text{N}_2)]\text{NO}_3$ (III). Characterization data follow. White powder. Yield: 47% (89 mg). NMR δ (^1H) 7.42–7.58 (m, 15H); 6.84 (s, 1H); 6.51 (br, 1H); 6.42 (d, 1H). δ (^{31}P) 28.2 ppm; m/z 567 $[(\text{Ph}_3\text{P})\text{Au}(\text{C}_6\text{H}_8\text{N}_2)]^+$. Anal. Calcd (%) for $\text{C}_{24}\text{H}_{23}\text{N}_3\text{O}_3\text{PAu}$: C, 45.8; H, 3.68; N, 6.68. Found (%): C, 45.6; H, 3.55; N, 6.56.

$[(\text{Ph}_3\text{P})\text{Au}(\text{C}_7\text{H}_{10}\text{N}_2)]\text{NO}_3$ (IV). Characterization data follow. White powder. Yield: 41% (79 mg). NMR δ (^1H) 8.33 (d, 2H); 7.42–7.58 (m, 15H); 6.49 (d, 2H); 3.11 (s, 6H). δ (^{31}P) 27.5 ppm; m/z 581 $[(\text{Ph}_3\text{P})\text{Au}(\text{C}_7\text{H}_{10}\text{N}_2)]^+$. Anal. Calcd (%) for $\text{C}_{25}\text{H}_{23}\text{N}_3\text{O}_3\text{PAu}$: C, 46.7; H, 3.92; N, 6.53. Found (%): C, 46.3; H, 3.80; N, 6.21.

DNA Melting Point Determination in the Presence and Absence of Gold Compounds I–IV. Calf thymus DNA (CT-DNA) solution (expressed as nucleotides) was prepared in 10 mmol L^{-1} NaClO_4 and dialyzed for 48 h. The 1 mmol L^{-1} stock solutions of the gold compounds were prepared in DMSO. A 100 $\mu\text{mol L}^{-1}$ DNA solution was incubated with the gold(I) compounds (I–IV) at various ratios ($r_i = 0$ –0.10; r_i being the ratio of compound per nucleotide) at 37 °C for 24 h. The maximum concentration of DMSO was 1% (v/v), and this amount was added to the $r_i = 0$ and incubated for 24 h. To avoid the formation of air bubbles during the experiment, the samples were degassed by stirring under vacuum for 5 min. The resulting melting curves were normalized, and the melting temperature was determined by sigmoidal curve fitting using Origin 8.0 software. Experiments were performed in triplicate.

Ethidium Bromide Interaction with DNA in the Presence and Absence of Gold Compounds I–IV. CT-DNA was prepared in buffer solutions containing 10 mmol L^{-1} PO_4^{3-} and 50 mmol L^{-1} NaCl (pH 7.4). The concentrations of nucleic acids (expressed as nucleotides) and ethidium bromide were determined spectrophotometrically using the following extinction coefficients: $\epsilon_{260} = 6000 \text{ M}^{-1} \text{ cm}^{-1}$ for CT-DNA¹⁶ and $\epsilon_{338} = 5680 \text{ M}^{-1} \text{ cm}^{-1}$ for ethidium bromide.^{17,18} Stock solutions of the CT-DNA incubated with the gold(I) compounds (I–IV) at an r_i of 0.1 (r_i being the ratio of compound per nucleotide) were prepared and incubated at 37 °C for 24 h. Varying amounts of ethidium bromide in the range 0–0.25 ethidium bromide per nucleotide were added to CT-DNA and CT-DNA treated with I–IV. The final concentration of CT-DNA in samples was 5 $\mu\text{mol L}^{-1}$. Fluorescence emission spectra were recorded on a Cary Eclipse (Varian) fluorimeter at 25 °C. Fluorescence was excited at $\lambda_{\text{ex}} = 525 \text{ nm}$ and registered at $\lambda_{\text{em}} = 600 \text{ nm}$. Spectra were recorded thrice and averaged. Because the absorbance of all samples at excitation wavelength was less than 0.05, the inner filter was disregarded.

Interaction with Model Amino Acids (*N*-Acetyl-L-cysteine). Gold(I) complexes II–IV were dissolved in 750 μL of CD_3CN to a final concentration of 20 mmol L^{-1} . An equivalent amount of *N*-acetyl-L-cysteine was dissolved separately in 750 μL of CD_3CN . The interaction of the compounds with each amino acid was evaluated by ^1H and ^{31}P NMR spectroscopy by mixing one solution of gold(I) compound and the amino acid at the time of the spectral acquisition. The formation of solid precipitate was observed prior to the transfer of the solution to the NMR tube. Centrifugation was used to separate solid particles when necessary. The NMR tubes were kept at 37 °C bath for spectral acquisition after 24, 48, and 72 h.

Interaction with *N*-Acetyl-tryptophan. Solutions of gold(I) complexes I–IV were prepared in acetonitrile to a final concentration of 7.5 mmol L^{-1} . A 10 mmol L^{-1} stock solution of *N*-acetyltryptophan was prepared in tris buffer 20 mmol L^{-1} pH 7.4. In a fluorescence cuvette, 3 mL of 5 $\mu\text{mol L}^{-1}$ solution of *N*-acetyltryptophan was titrated with volumes of 20 μL of the stock solution of the gold(I) compound, and the fluorescence emission was measured in a range 300–450 nm, with an excitation wavelength of 280 nm and a detector voltage of 750 V. The temperature was kept at 25 °C during the experiment. The K_a values were determined from Eadie Hofstee plots and were determined from an average of 3 trials using the following equation: $\Delta F = (K_a)^{-1} \Delta F / [\text{quencher}] + \Delta F_c$.

Interaction with Zinc Fingers. Zinc fingers (ZFs) were prepared for circular dichroism (CD) and ESI-MS analysis according to the following procedure: 0.5 mg of the apo-peptide was dissolved in 0.5 mL of degassed water, and the pH was then adjusted to 7.4 with NH_4OH . The concentration based on the isotopic mass was 0.3 mmol L^{-1} . A 10 mmol L^{-1} stock solution of zinc acetate in degassed water was prepared, and 19.3 μL of this solution was added to the peptide for a final molar ratio of 1:1.3 (peptide/ Zn^{2+}). The solution was then incubated at 37 °C for 2 h and could be kept in freezer as a stock for 72 h. Stock solutions of the gold(I) compounds were prepared in acetonitrile for a final concentration of 10 mmol L^{-1} . For general ESI-MS or CD evaluations the molar ratio 1:1.3 (ZF/Au) was used. Titrations for CD analysis were made adding different volumes of this stock solution of compounds to a stock solution of the ZF and the final molar ratios reported. For NMR purposes the stock solutions of the peptide, zinc acetate, and gold compounds were prepared in the same conditions described above using deuterated solvents D_2O and CD_3CN . pH adjustments were made using NaOD . The molar ratio was 1:1.3 (peptide/ Zn^{2+}) and 1:1.3 (ZF/ Au^+).

Cytotoxicity Assays. HCT116, A2780, and MCF7s cell lines were used in this study and maintained according to published procedures.^{19,20} The IC_{50} values were calculated similar to that described previously.²¹ In brief, cells were cultured in RPMI (Gibco, Carlsbad, CA), 5% FBS, 5% BCS, 0.25% penicillin/streptomycin. Cells were routinely passaged at 80–90% confluence. For the MTT assay, cells were plated at a density of 5000 cells per well in a 96-well plate and incubated overnight at 37 °C in a 5% CO_2 atmosphere. Cells were treated with a varying drug concentration for 96 h. After drug removal, cells were incubated with MTT (3-(4,5-dimethyl-2-thiazolyl)-2,5-diphenyl-2H-tetrazolium bromide) (0.5 mg/mL in RPMI) for 3 h. The excess MTT was then removed. The dye was dissolved in 100 μL of DMSO (Sigma; St Louis, MO), and absorbance was read at 540 nm.

Cell Uptake. HCT116 cells were plated in 10 cm dishes at 5×10^5 cells per dish and allowed to attach overnight. The cells were then treated with IC_{90} concentrations of each compound. After 3 and 6 h the medium was collected in 15 mL falcon tubes. The cells were removed from the dish with trypsin and then centrifuged for 3 min at 1000g at 4 °C. The medium was removed, the cell pellet was washed three times with cold PBS, and the cells were counted. The samples were digested by addition of 1 mL of fuming hydrochloric acid. The acid content was diluted by the addition of 1 mL of deionized water. Analysis of the gold content was performed on a Varian ICP-MS using $\text{H}[\text{AuCl}_4]$ for the analytical curve. Standards and blank were prepared similarly. Plates were prepared in duplicate. The results shown are a combination of three different experiments.

Cell Cycle Arrest. HCT 116 cells were plated in Petri dishes and allowed to settle in the incubator overnight. The next day, the gold compounds were added from a 10 mmol L^{-1} stock solution in DMSO to the final IC_{90} concentration. To the untreated control, the maximum volume of DMSO added was 1% v/v the final amount. The cells were incubated for 24–48 h. Cells were detached using trypsin (Gibco), washed twice with PBS, and suspended in propidium iodide staining solution (50 $\mu\text{g mL}^{-1}$ propidium iodide, 0.1% Triton-X in PBS) containing RNase A (200 U mL^{-1}). Cell cycle analysis was done after 15 min incubation on a FACSsort flow cytometer (Becton Dickinson).

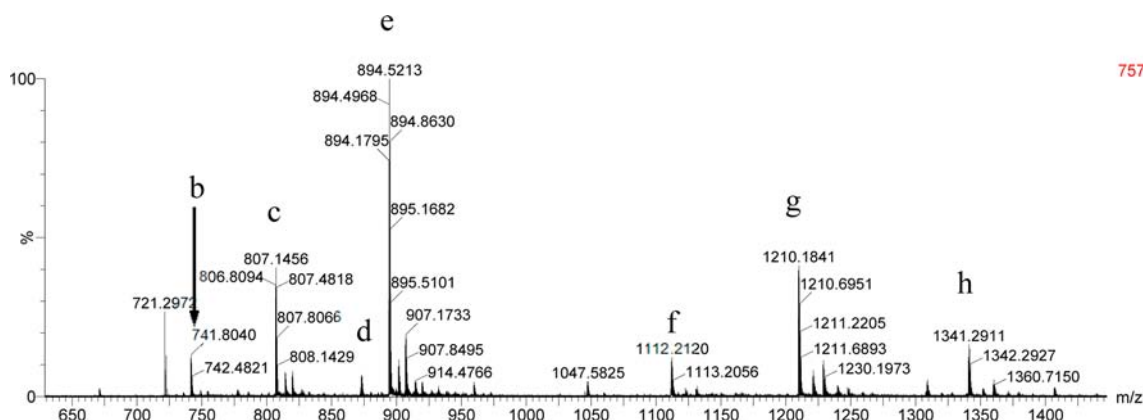


Figure 2. ESI-MS full scan (positive mode) of reaction between **IV** $[(\text{PPh}_3)_2\text{Au}(\text{DMAP})]^+$ and ZF NCp7 immediately upon incubation. The species at m/z 721.29 is assigned to $[\text{Au}(\text{PPh}_3)_2]^+$. Other species are as follows: (b) $[\text{apoNCp7}]^{3+}$ m/z 741.8, (c) $[\text{AuF}]^{3+}$ m/z 807.15, (d) $[\text{Au}_2\text{F}]^{3+}$ m/z 873.65, (e) $[\text{apoNCp7}\text{-}\{\text{Au}(\text{PPh}_3)_2\}]^{3+}$ m/z 894.52, (f) $[\text{apoNCp7}]^{2+}$, (g) $[\text{AuF}]^{2+}$ m/z 1210.18, (h) $[\text{apoNCp7}\text{-}\{\text{Au}(\text{PPh}_3)_2\}]^{2+}$ m/z 1341.29. apoNCp7 (or F) refers to the ZF peptide with loss of Zn^{2+} . (apoNCp7 represents the apo-peptide of C-terminal HIV NCp7 zinc finger; $[\text{AuF}]$, $[\text{Au}_2\text{F}]$ represent Au complexed to apoNCp7.)

RESULTS AND DISCUSSION

The N-heterocycles are good σ -donor and π -acceptor groups and can modulate the properties of the *trans* phosphine. The compounds were characterized by elemental analysis; ^1H , ^{13}C , and ^{31}P NMR spectroscopy (Supporting Information Figure S1); mass spectrometry; and electronic spectroscopy, Table 1.

The ^{31}P NMR signals of all compounds were shifted 3–4 ppm upfield compared to the $[(\text{PPh}_3)_2\text{AuCl}]$ starting material (30.8 ppm), consistent with a shielding of this atom, Supporting Information Figure S1. The peaks are broad which could be due to some line broadening or possible exchange between discrete $[(\text{PPh}_3)_2\text{AuL}]$ complexes and a statistical mixture of $[\text{Au}(\text{PPh}_3)_2]^+$ and $[\text{AuL}_2]^+$. The former ion but not the latter is seen in the mass spectra. In the ^1H NMR spectrum, for **II**, the *ortho*-(2,6) protons of the pic ligand are shifted downfield by 0.24 ppm, and the CH_3 group is likewise shifted downfield by 0.14 ppm compared to free ligand. The *para*-protons are obscured by the PPh_3 resonance. In contrast, the *ortho*-protons of **IV** are only moderately affected (0.1 ppm upfield), but the NMe_2 ligands undergo a significant deshielding of 0.64 ppm consistent with donation of electron density to the Au–P bond. In this case the *meta*-(3,5) protons are also shifted downfield by 0.30 ppm.

The exocyclic amine and the pyridine nitrogen represent two possible binding sites for ligand L3. The ^{31}P NMR shift is consistent with binding through the pyridine nitrogen. The singlet of proton 3 is shifted downfield by 0.52 ppm while the pair of doublets at 6.46 and 7.94 ppm in the ^1H NMR spectrum of the L3 corresponding to the protons 5 and 6 are shifted upon coordination to 7.50 ppm (obscured within Ph_3P multiplet) and 6.51 ppm, respectively. The C(2)– NH_2 protons undergo a downfield shift of 2.09 ppm, suggesting the amine nitrogen is uncoordinated. This was further confirmed by disappearance of the signal upon addition of D_2O . In the ^{13}C NMR C(2)– NH_2 does not shift whereas the C6 signal is shifted downfield by 5.06 ppm. Overall, the pyridine N represents the most likely binding site.

In the ESI-MS of the compounds, the molecular ion of **I** is not observed, and the main peak corresponds to that of the disproportionation product $[\text{Au}(\text{PPh}_3)_2]^+$. In contrast, for $[(\text{PPh}_3)_2\text{AuL}]^+$ all species show the molecular ion, and also the loss of the N-heterocycle ligand (L) and rearrangements

producing the $[\text{Au}(\text{PPh}_3)_2]^+$ ion, Table 1. The intensity of the $[\text{Au}(\text{PPh}_3)_2]^+$ ion varies with L: the least intense occurs in the spectrum of strongest base, 4- Me_2N -pyr (**IV**), which also has the sharpest ^{31}P NMR spectrum. In the case of **II**, L = 4-picoline, mass spectra show peaks at m/z of 459 for $[\text{Au}(\text{PPh}_3)_3]^+$ and at $m/z = 500$ corresponding to $[\text{Au}(\text{PPh}_3)(\text{CH}_3\text{CN})]^+$ (from solvent) indicating substitution lability of this ligand, Supporting Information Figure S2. It is of interest that this compound also shows the broadest ^{31}P NMR spectrum suggesting susceptibility to rearrangement, depending on donor strength of ligand.

Potentiometric studies of **II** and **IV** in $\text{H}_2\text{O}/\text{CH}_3\text{CN}$ (1:5) give pK_a values for pyridine protonation of 4.31 and 8.42, respectively, Supporting Information Figure S3. These are lower than literature values in H_2O of 5.99 and 9.70, respectively. Interestingly, the kinetics of L (N-heterocycle) substitution by Cl^- in $\text{AuCl}_3\text{L} + \text{Cl}^- \rightarrow [\text{AuCl}_4]^- + \text{L}$ showed a linear relationship between the basicity of the leaving group and the reactivity (expressed as the logarithm of the second order rate constant) with respect to chloride substitution, where the entering group is acting essentially as a σ -bonding nucleophile.²² These trends may also be reflected in the differential susceptibility of **II–IV** to rearrangement to the $[\text{Au}(\text{PPh}_3)_2]^+$ ion and the electron donation to the Au(I) center as evidenced by NMR parameters. A second inflection point in the potentiometric titration at approximately 3.4–3.7 is also present in **I** and is assigned to the protonation of the phosphine ligand. These values are broadly consistent with those reported in the literature for tertiary phosphines and diphosphines, although the solvent conditions vary greatly.^{23,24}

Reactivity with Biomolecules. Melting points of calf thymus DNA (CT-DNA) after incubation with the complexes in the molar ratios (r_i) 0, 0.01, 0.03, 0.05, 0.075, and 0.1 for 24 h showed little variation, Supporting Information Table S1. Competition assays of the DNA–ethidium bromide intercalator interaction also showed little difference in fluorescence quenching confirming that the DNA is unlikely to be the principal target for these compounds, Supporting Information Figure S4.^{25,26}

As stated, protein thiols and selenols are indicated as biological targets of Au(I). The reaction of **II** and **IV** with *N*-acetylcysteine (*N*-AcCys, 1:1 stoichiometry) showed immediate changes in the ^{31}P NMR spectrum with significant shifts from

30 to 38 ppm followed by an immediate white precipitate, consistent with displacement of L followed by coordination of a sulfur donor ligand, giving a P–Au–S coordination unit, Supporting Information Figure S5.²⁷ Early studies on antiarthritic gold complexes suggested a plausible mode of action as inhibition of zinc fingers through metal ion displacement.^{8,9} A number of Au(I) and Au(III) compounds have been studied for their interactions with zinc fingers. Continuing our systematic studies on the chemistry of coordination compounds with zinc fingers,²⁸ we studied the reactions of the series with two representative zinc finger peptides: the C-terminal Cys₃His finger of HIV Nucleocapsid 7 (ZFNCP7) and finger 3 of the Cys₂His₂-based Sp1 transcription factor.

The ESI-MS (positive mode) of the reaction between [(Ph₃P)Au(DMAP)]⁺, **IV**, and ZF NCp7 immediately upon incubation shows a number of new peaks. The most prominent are those at 894.52 (3+) and 1341.29 *m/z* (2+) corresponding to the [apoNCp7-{Au(PPh₃)}]ⁿ⁺ ion. Other notable species besides unreacted zinc finger itself correspond to [AuapoNCp7, AuF]³⁺ and [Au2apoNCp7, Au₂F]³⁺ species caused by zinc ejection and free peptide itself (apoNCp7, 15% intensity), Figure 2. The [apoNCp7-{Au(PPh₃)}] species persists even up to 78 h of reaction time (Supporting Information Figure S6). The MS/MS dissociation of the 894.52 (3+) species gave new peaks corresponding to free phosphine [PPh₃ + H]⁺ and the previously observed “gold finger” [AuF]³⁺ species (data not shown). The results are consistent with, first, displacement of the DMAP ligand and formation of an Au(PPh₃) adduct with Zn displacement, followed by loss of PPh₃ to give [AuF]. Similar spectra are observed for the chloride derivative and also for the 4-picoline (**II**) and 2-amino-4-picoline analogues (**III**) (Supporting Information Figure S7). The MS–MS of the [Au₂F]³⁺ peak at *m/z* 873.65 is remarkably resistant to fragmentation, suggesting by definition a very stable structure (Supporting Information Figure S8).

The ³¹P NMR spectrum of [(PPh₃)Au(DMAP)]⁺, **IV**, incubated with ZF NCp7 gave two new peaks at 32.92 and 34.35 ppm representing shifts of 6.32 and 7.56 ppm, respectively, from the complex, Figure 3. The species is stable over time [water pH 7.4 containing 10% (v/v) acetonitrile] with no signals detected assignable to PPh₃O or free PPh₃. The chemical shifts are entirely consistent with literature values of

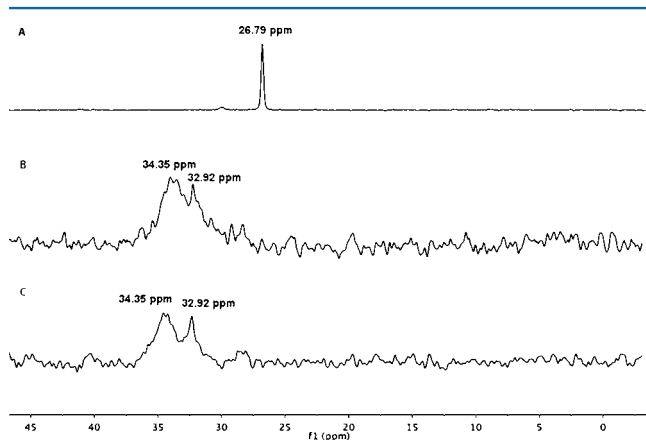


Figure 3. ³¹P NMR spectra of compound **IV** and ZFNCP7: (A) compound **IV**, (B) **IV** + ZFNCP7 immediately after mixing, and (C) **IV** + ZFNCP7 at time 7 days.

auranofin [Au(PEt₃)(S-thioglucose)] and the reaction products of [AuCl(PEt₃)] with cysteine and protein thiolate residues in serum albumin.^{27,29,30} The presence of two peaks implies at least two species, which is reasonable given the presence of three thiolate ligands (Cys) and one histidine residue (His) in the peptide sequence. Further, the broadness of the peaks first suggests different microenvironments and perhaps some conformational flexibility.

Zinc finger cysteinates vary in chemical reactivity, and nucleophilicity is very dependent on the nature of the Zn-binding core. The Zn-Cys49 thiolate of NCp7 is one of the residues most susceptible to electrophilic attack.³¹ To examine this point further we compared the reactivity of ZFNCP7 with that of zinc finger 3 of the Sp1 transcription factor (Sp1F3). Previous studies with aurothiomalate and Sp1F3 showed rapid formation of [AuapoSp1F3, (or AuF3)] with indications of an ordered structure.¹⁰ (apoSp1F3 is the apo-peptide of Finger 3 of transcription factor Sp1; [AuF3], [Au₂F3] represent Au complexed to apoSp1.)

Incubation of the Sp1F3 with **IV** again showed a number of species but with significantly reduced intensity for any putative {Au(Ligand)}-apoSp1 species. The ejection of zinc is quick, and the dominant species in all cases (**I–IV**) shows a set of peaks at 891.74 (4+) and 1188.32 (3+) corresponding to [AuapoSp1F3]ⁿ⁺. The presence of [Au₂Sp1F3, Au₂F3]ⁿ⁺ (3+ and 4+) is also seen, Figure 4 and Supporting Information Figure S9. No apoSp1F3-{Au(PPh₃)} was observed for any of these compounds. However, for compound **IV** only, peaks at 1006 and 1341 *m/z* (charge 4+ and 3+, respectively) correspond to a mass of [apoSp1F3-{(PPh₃)Au₂}] implying the presence of one coordinated Au(PPh₃) unit and one Au devoid of starting ligands (Figure 4). The reaction with the Sp1 finger is thus more ligand-specific since no evidence for any equivalent Au(PPh₃) species is seen for compounds **I–II** containing as ligands L1 = Cl[−] or L2 = 4-picoline (Supporting Information Figure S9). The prototypical [Au(III)Cl(dien)]²⁺ reacts readily with the C-terminal zinc finger of the HIV nucleocapsid Cys₃His zinc finger (NCp7) producing Au₂F and Au₄F species, as monitored by ESI-MS.¹² Thus, the nature of these reactions depends both on the compound and leaving group (Cl[−] or substituted pyridine) as well as the coordination sphere of the zinc finger itself (Cys₃His or Cys₂His₂).

Conformational changes upon binding were further analyzed by circular dichroism spectroscopy (CD) to confirm these differences. The interactions of **I** and **IV** with ZFNCP7 and Sp1F3 are shown in Figure 5. No significant differences were found for compounds **II** and **III** (data not shown). The apoNCp7 and apoSp1F3 present typical random coil spectra with a negative ellipticity centered at 195–200 nm.^{12,32} Zn²⁺ coordination to the peptide in a tetrahedral environment decreases the intensity with a slight red shift at 200–210 nm and a positive signal at 190 nm indicating a more α -helical conformation, Figure 5A,B.

For ZFNCP7 reaction with **I** and **IV**, unusual and shapeless CD spectra were produced. In the case of the reaction of [AuCl(dien)]²⁺ with ZFNCP7, the negative ellipticity is decreased in the range 190–200 nm and the minimum is shifted in comparison to apoNCp7.¹² CD spectra do represent the sum of conformations present, but it is expected that the conformation of the peptide will change upon coordination of gold(I) in a linear geometry rather than the tetrahedral geometry of Zn²⁺. The presence of different species in solution, apoNCp7-{Au(PPh₃)}, AuF, and AuF₂, with different con-

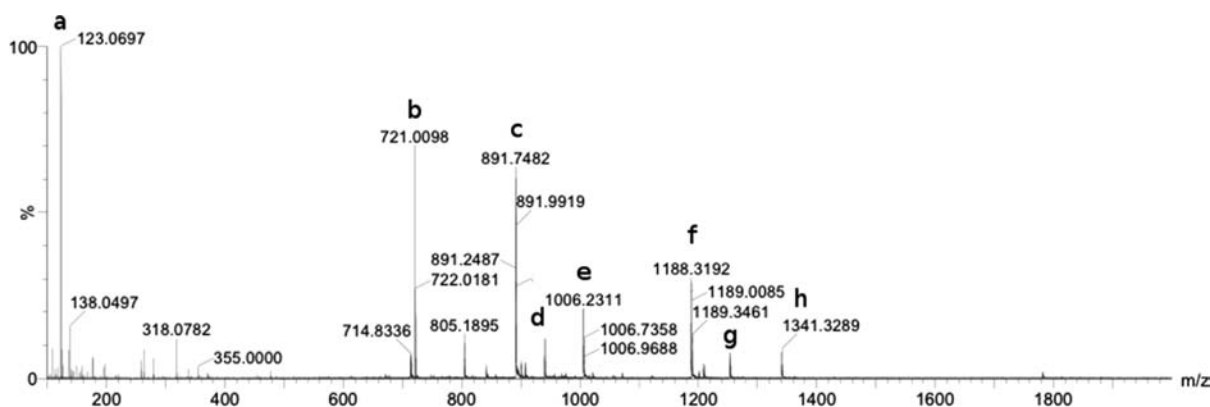


Figure 4. ESI-MS full scan (positive mode) of the reaction between $[(\text{PPh}_3)\text{Au}(\text{DMAP})]^+$ and Sp1F3 immediately upon incubation. Species (a) $[\text{DMAP} + \text{H}^+]^+$, (b) $[\text{Au}(\text{PPh}_3)_2]^+$, (c) $[\text{Au}-\text{apoSp1F3}, \text{AuF}_3]^{4+}$, (d) $[\text{Au}_2-\text{apoSp1F3}, \text{Au}_2\text{F}_3]^{4+}$, (e) $[\text{apoSp1F3}-\{(\text{PPh}_3)\text{Au}_2\}]^{4+}$, (f) $[\text{AuF}_3]^{3+}$, (g) $[\text{Au}_2\text{F}_3]^{3+}$, (h) $[\text{apoSp1F3}-\{(\text{PPh}_3)\text{Au}_2\}]^{3+}$. apoSp1F3 or F3 refers to the zinc finger peptide with loss of Zn^{2+} .

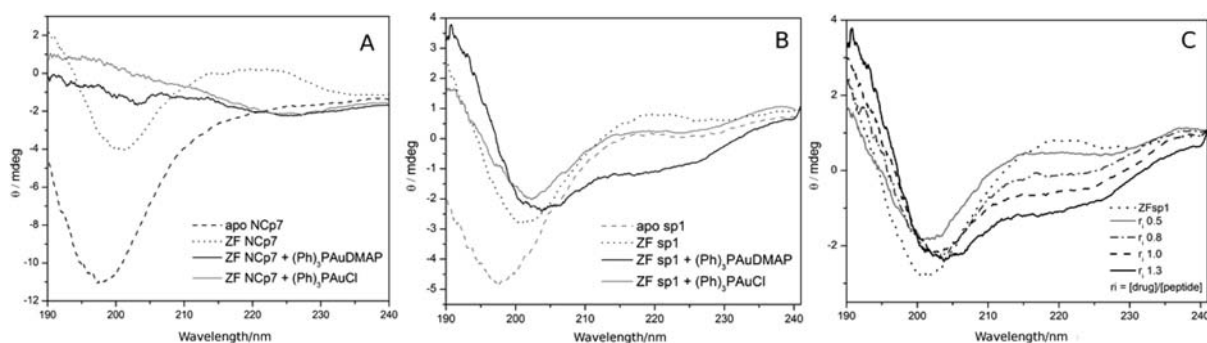


Figure 5. CD spectra of apo-peptides, zinc fingers, and zinc finger + Au(I) drugs (I and IV): (A) N Cp7, (B) Sp1F3, (C) Sp1F3 + IV titration.

formations, obviates against observation of well-defined signals especially as the $\text{Au}(\text{PPh}_3)$ adduct is the dominant species. However it is clear that the peptide conformation changed and no free apoN Cp7 is detected as the main species in solution, Figure 5A.

In contrast, the Sp1F3 showed a concentration-dependent alteration where the structure is clearly ordered but distinct from the starting Sp1F3 or free peptide (apoSp1F3), Figure 5B. The chloride compound, I, presented a slight decrease in the negative and positive ellipticity, being consistent with previously reported results.^{11,12} Compound IV showed a red shift, an increase in the positive signal in the range 190–195 nm and a significant increase in the positive signal in the range 210–220 nm. Interestingly, the changes for IV are concentration-dependent, and the presence of a putative isodichroic point at ~ 200 nm suggests that the same products or a mixture of products is produced. The results for the Sp1 finger are generally consistent with those previously reported for Au(I) compounds and zinc finger model peptides. Binding of $[\text{AuCl}(\text{PEt}_3)]$ to consensus sequences for Cys_2His_2 , Cys_3His , and Cys_4 models showed a stoichiometry of $1\text{Au}:2\text{Cys}$ binding for all peptides, and the gold fingers produced were more ordered than free peptide but again conformationally distinct from the canonical Zn finger structure.¹¹ As stated, CD spectroscopy showed differences in conformation upon treatment of zinc fingers with aurothiomalate, with zinc ejection and formation of Au peptides, resulting in inhibition of the DNA binding of the two model Cys_2His_2 transcription factors TFIIIA and Sp1.¹⁰

The presence of the aromatic residue tryptophan (Trp) in the C-terminal N Cp7 is a potential source of differentiation for

reactivity of the zinc fingers with Au compounds through molecular recognition and targeting with π -stacking ligands.^{32,33} “Noncovalent” association with tryptophan and ZFN Cp7 has been confirmed for $[\text{Pt}(\text{dien})(\text{nucleobase})]^{2+}$ (nucleobase = 9-EtGua, 1-MeCyt).^{33,34} Pyridine ligands may also of course engage in π stacking interactions. Assessment of stacking with ZFN Cp7 was not feasible due to the rapid ejection of Zn^{2+} , but use of *N*-acetyl-tryptophan indicated possible π stacking with IV, enhanced over free DMAP ligand, L4, alone (Table 2). The Try-RNA(DNA) interaction is a critical feature of N Cp7 function.^{35–37}

Table 2. Association Constants for Au Compounds with *N*-AcTryptophan by Fluorescence Quenching^a

quencher	K_a ($\times 10^3 \text{ M}^{-1}$)	$\pm \text{SD}$ ($\times 10^3$)
I	<i>b</i>	
II	2.55	0.01
L2	<i>b</i>	
IV	25.0	0.20
L4	3.19	0.01

^aThe K_a was determined from Eadie Hofstee plots and determined from an average of 3 trials using the equation $\Delta F = (K_a)^{-1} \Delta F / [\text{quencher}] + \Delta F_c$. ^bNo quenching observed

Cellular Effects. All complexes show strong antiproliferative effects *in vitro* against human colon carcinoma (HCT116), human ovarian carcinoma (A2780), and human breast carcinoma (MCF7), Table 3 and Supporting Information Figure S10. All compounds displayed greater cytotoxicity than cisplatin control in the human colon and ovarian tumor lines

Table 3. IC₅₀ Values for Gold(I) Compounds in HCT116, A2780, and MCF7 Tumorigenic Cell Lines

compd	IC ₅₀ /μmol L ^{-1a}					
	A2780		HCT116		MCF7	
I	0.303	±0.068	1.478	±0.430	2.467	±0.051
II	0.324	±0.061	1.269	±0.248	2.245	±0.140
III	0.319	±0.085	1.226	±0.075	2.265	±0.065
IV	0.238	±0.038	0.914	±0.170	2.271	±0.078
cisplatin ^b	2.31	±0.06	7.6	±1.70	4.8	±0.80

^aValues are an average of three different experiments. Free ligands show no cytotoxicity at <25 μmol L⁻¹ under identical conditions.

^bValues for cisplatin performed under identical conditions.

and equivalent cytotoxicity in the breast cancer cell line. No significant differences are observed among I–IV themselves with only slight differences in values in any individual cell line. Extensive surveys of cytotoxicity and biological activity of Au(I)-phosphine complexes have emphasized variation of the phosphine ligand.^{15,38}

Intracellular gold accumulation studies showed the highest accumulation for the neutral I compared to the cationic complexes, Figure 6. This similarity may reflect rapid

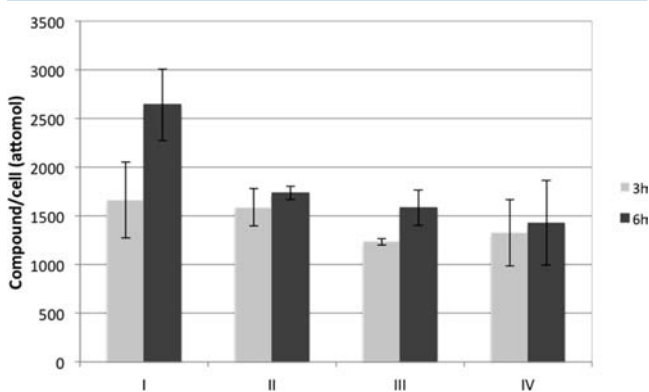


Figure 6. Bar graphs showing the total gold accumulation for HCT116 cells treated with compounds I, II, III, and IV.

displacement of either Cl⁻ or L by intracellular thiol. However, the fact that accumulation levels for II–IV are similar at 3 and 6 h implies a more rapid uptake than I and a possible carrier-mediated uptake if saturation is achieved at these early time points. Cellular accumulation of Au(I)-diphosphine and N-heterocycle carbene complexes may be modulated through lipophilicity of the ligand, leading to development of Au(I) compounds as mitochondrial poisons.^{1,39} Cell cycle effects on HCT116 cells by flow cytometry staining showed a significant increase in the percentage of the cells in the G1 phase compared to the control set, suggesting induction of cell growth inhibition by elongation of the G1 phase in the cell cycle, Supporting Information Figure S11.

CONCLUSIONS

The set of [(PR₃)Au(I)(L)]⁺ (L = N-heterocyclic) compounds represents a new series of Au(I) compounds with interesting biological activity. Their interaction with N-acetyl-cysteine in acetonitrile showed displacement of the planar amine with precipitation of insoluble compounds. Gold phosphine-imido complexes have been reported for their antiarthritic activity,⁴⁰

and other P–Au–N compounds have been reported in isolation.^{41,42}

As stated, the inherently “soft” nature of Au(I) has long suggested thiol interactions as possible modes of action of these drugs. The studies reviewed here confirm the suggestions that zinc fingers are also suitable receptors. In this study we show for the first time that the interactions may be modulated by both the nature of the ligand and the zinc finger coordination motif. This study represents the first observation of gold-(ligand) interactions on these biologically important zinc finger proteins: all other examples have had Au stripped of all ligands. (PR₃)Au-protein species have been confirmed in other proteins such as HAS^{2,27,29,30} and Ubiquitin,⁴¹ but these generally are not as thiol-rich as the zinc fingers. Some organometallic Au(III) compounds also show Au(ligand)-protein adducts by mass spectrometry.⁴³ The apoNCp7-Au(PPh₃) species is remarkably long-lived as assessed by both MS and NMR studies, and it is further noteworthy that the Au₂apoNCp7 species (Au₂F, see Figure 2) produced is also remarkably stable: it does not fragment under MS/MS conditions, Supporting Information Figure S11. The chemistry is best described in Figure 7. Given evidence of multiple (PPh₃)Au–S(cysteine)

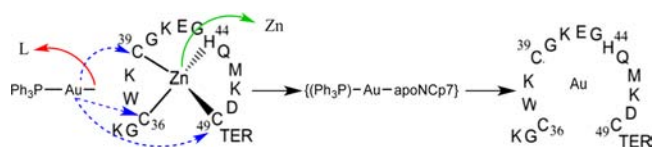


Figure 7. Stepwise coordination of gold(I) drugs and zinc ejection.

species no specific binding sites should be assigned, but the AuF species would be expected to be linear S–Au–S while the Au₂F species can be easily envisaged as a Au₂Cys₃ system arising from monodentate and bridging cysteinates.

The chemistry described here suggests [(PR₃)AuL]⁺ may be complementary to agents such as iodoacetate and N-ethyl-maleimide as probes of zinc finger structure and function.⁴⁴ The susceptibility to oxidative attack on the cysteine ligands also suggests approaches to the design of electrophilic agents for inactivation of zinc finger medicinal targets.²⁸ The full 2-finger HIV NCp7 is an attractive drug target for inhibition of HIV infectivity.^{45–47} Electrophilic agents target NCp7 causing Zn²⁺ ejection, resulting in loss of native protein structure and nucleic acid binding capacity, effectively causing disruption of virus replication. A consideration for any anti-HIV drug potential is selectivity among zinc fingers. Notable examples are DIBA-1, dithiane, and ADA which show some selectivity of attack on NCp7 without significantly affecting other cellular proteins such as poly(ADP-ribose) polymerase (PARP) and the Sp1 and GATA-1 transcription factors.⁴⁸ The results presented here confirm the value of coordination chemistry for systematic modulation of protein chemical behavior. The series presented here allows systematic (electronic, steric, lipophilicity) variations of “carrier” group PR₃ and “leaving” group L in modulation of biological parameters of cellular accumulation and cytotoxicity, similar to the mechanistic concept for cisplatin anticancer agents. It is of considerable interest that auranofin itself has been shown to inhibit viral load in simian virus.⁴⁹ The results presented here may well be relevant to these observations. Systematic study of the potential of gold compounds against this HIV target is warranted.⁵⁰

■ ASSOCIATED CONTENT

■ Supporting Information

^1H and ^{31}P NMR spectra, ESI-MS, pH titrations, and species distribution of compounds I–IV, ethidium bromide fluorescence assay and table of DNA melting temperatures, ^{31}P NMR spectra of II and IV and their interaction with N-AcCysteine, ESI-MS spectra of reactions of I–IV with zinc finger proteins, cytotoxicity curves, and cell cycle effects of I–IV. This material is available free of charge via the Internet at <http://pubs.acs.org>.

■ AUTHOR INFORMATION

Corresponding Author

*E-mail: nparrell@vcu.edu.

Author Contributions

All authors have given approval to the final version of the manuscript.

Notes

The authors declare no competing financial interest.

■ ACKNOWLEDGMENTS

This work was financially supported by NSF CHE 1058726. The authors acknowledge the award of a scholarship to C.A. by Coordination for the Improvement of High-Level Personnel (CAPES) Process 2276-11-9. We thank K. Nelson and K. Knitter for mass spectra.

■ REFERENCES

- Berners-Price, S. J.; Filipovska, A. *Metallomics* **2011**, *3*, 863–873.
- Shaw, C. *Chem. Rev.* **1999**, *99*, 2589–2600.
- Tiekink, E. R. *Crit. Rev. Oncol. Hematol.* **2002**, *42*, 225–248.
- Bindoli, A.; Rigobello, M. P.; Scutari, G.; Gabbiani, C.; Casini, A.; Messori, L. *Coord. Chem. Rev.* **2009**, *253*, 1692–1707.
- Fricker, S. P. *Metallomics* **2010**, *2*, 366–377.
- De Luca, A.; Hartinger, C. G.; Dyson, P. J.; Lo Bello, M.; Casini, A. *J. Inorg. Biochem.* **2013**, *119*, 38–42.
- Ilari, A.; Baiocco, P.; Messori, L.; Fiorillo, A.; Boffi, A.; Gramiccia, M.; Di Muccio, T.; Colotti, G. *Amino Acids* **2011**, *42*, 803–811.
- Handel, M. L.; Watts, C. K.; Day, R. O.; Sutherland, R. L. *Proc. Natl. Acad. Sci.* **1995**, *92*, 4497–4501.
- Handel, M. L.; deFazio, A.; Watts, C. K.; Day, R. O.; Sutherland, R. L. *Mol. Pharmacol.* **1991**, *40*, 613–618.
- Larabee, J. L.; Hocker, J. R.; Hanas, J. S. *Chem. Res. Toxicol.* **2005**, *18*, 1943–1954.
- Franzman, M. A.; Barrios, A. M. *Inorg. Chem.* **2008**, *47*, 3928–3930.
- De Paula, Q. A.; Mangrum, J. B.; Farrell, N. P. *J. Inorg. Biochem.* **2009**, *103*, 1347–1354.
- Mendes, F.; Groessl, M.; Nazarov, A. A.; Tsybin, Y. O.; Sava, G.; Santos, I.; Dyson, P. J.; Casini, A. *J. Med. Chem.* **2011**, *54*, 2196–2206.
- Gutz, I. G. R. *CurTiPot - pH and Acid-Base Titration Curves: Analyses and Simulation Software, Version 3.6.1*, <http://www2.iq.usp.br/docente/gutz/Curtipot.html>, 1992–2013.
- Karver, M. R.; Krishnamurthy, D.; Kulkarni, R. A.; Bottini, N.; Barrios, A. M. *J. Med. Chem.* **2009**, *52*, 6912–6918.
- Wells, R. D.; Larson, J. E.; Grant, R. C.; Shortle, B. E.; Cantor, C. R. *J. Mol. Biol.* **1970**, *54*, 465–497.
- Lepecq, J.-B.; Paoletti, C. *J. Mol. Biol.* **1967**, *27*, 87–106.
- Winkle, S. A.; Rosenberg, L. S.; Krugh, T. R. *Nucleic Acids Res.* **1982**, *10*, 8211–8223.
- Kelland, L. R.; Jones, M.; Abel, G.; Valenti, M.; Gwynne, J.; Harrap, K. R. *Cancer Chemother. Pharmacol.* **1992**, *30*, 43–50.
- Kelland, L. R.; Barnard, C. F.; Mellish, K. J.; Jones, M.; Goddard, P. M.; Valenti, M.; Bryant, A.; Murrer, B. A.; Harrap, K. R. *Cancer Res.* **1994**, *54*, 5618–5622.
- Hegmans, A.; Qu, Y.; Kelland, L. R.; Roberts, J. D.; Farrell, N. *Inorg. Chem.* **2001**, *40*, 6108–6114.
- Cattalini, L.; Tobe, M. L. *Inorg. Chem.* **1966**, *5*, 1145–1150.
- Berners-Price, S. J.; Norman, R. E.; Sadler, P. J. *J. Inorg. Biochem.* **1987**, *31*, 197–209.
- Allman, T.; Goel, R. G. *Can. J. Chem.* **1982**, *60*, 716–722.
- McKeage, M.; Maharaj, L.; Berners-Price, S. *Coord. Chem. Rev.* **2002**, *232*, 127–135.
- Mirabelli, C. K.; Sung, C.-M.; Zimmerman, J. P.; Hill, D. T.; Mong, S.; Crooke, S. T. *Biochem. Pharmacol.* **1986**, *35*, 1427–1433.
- Coffer, M.; Shaw, C.; Eidsness, M.; Watkins, J.; Elder, R. *Inorg. Chem.* **1986**, *25*, 333–339.
- Quintal, S. M.; dePaula, Q. A.; Farrell, N. P. *Metallomics* **2011**, *3*, 121–139.
- Roberts, J.; Xiao, J.; Schleisman, B.; Parsons, D.; Shaw, C. *Inorg. Chem.* **1996**, *35*, 424–433.
- Malik, N. A.; Sadler, P. J. *Biochem. Soc. Trans.* **1979**, *7*, 731–732.
- Maynard, A.; Covell, D. J. *Am. Chem. Soc.* **2001**, *123*, 1047–1058.
- Quintal, S.; Viegas, A.; Erhardt, S.; Cabrita, E. J.; Farrell, N. P. *Biochemistry* **2012**, *51*, 1752–1761.
- Anzellotti, A. I.; Liu, Q.; Bloemink, M. J.; Scarsdale, J. N.; Farrell, N. *Chem. Biol.* **2006**, *13*, 539–548.
- Anzellotti, A. I.; Ma, E. S.; Farrell, N. *Inorg. Chem.* **2005**, *44*, 483–485.
- De Guzman, R. N. *Science* **1998**, *279*, 384–388.
- Morellet, N.; Déméné, H.; Teilleux, V.; Huynh-Dinh, T.; de Rocquigny, H.; Fournié-Zaluski, M.-C.; Roques, B. P. *J. Mol. Biol.* **1998**, *283*, 419–434.
- Bourbigot, S.; Ramalanjaona, N.; Boudier, C.; Salgado, G. F. J.; Roques, B. P.; Mély, Y.; Bouaziz, S.; Morellet, N. *J. Mol. Biol.* **2008**, *383*, 1112–1128.
- Mirabelli, C. K.; Johnson, R. K.; Hill, D. T.; Faucette, L. F.; Girard, G. R.; Kuo, G. Y.; Sung, C. M.; Crooke, S. T. *J. Med. Chem.* **1986**, *29*, 218–223.
- Hickey, J. L.; Ruhayel, R. A.; Barnard, P. J.; Baker, M. V.; Berners-Price, S. J.; Filipovska, A. *J. Am. Chem. Soc.* **2008**, *130*, 12570–12571.
- Berners-Price, S.; DiMartino, M.; Hill, D.; Kuroda, R.; Mazid, M.; Sadler, P. *Inorg. Chem.* **1985**, *24*, 3425–3434.
- Serratrice, M.; Edefe, F.; Mendes, F.; Scopelliti, R.; Zakeeruddin, S. M.; Graetzel, M.; Santos, I.; Cinellu, M. A.; Casini, A. *Dalton Trans* **2012**, *41*, 3287–3293.
- Travnicek, Z.; Starha, P.; Vanco, J.; Silha, T.; Hosek, J.; Suchy, P., Jr.; Prazanova, G. *J. Med. Chem.* **2012**, *55*, 4568–4579.
- Gabbiani, C.; Casini, A.; Kelter, G.; Cocco, F.; Cinellu, M. A.; Fiebig, H. H.; Messori, L. G. *Metallomics* **2011**, *3*, 1318–1323.
- Krizek, B. A.; Amann, B. T.; Kilfoil, V. J.; Merkle, D. L.; Berg, J. M. *J. Am. Chem. Soc.* **1991**, *113*, 4518–4523.
- De Clercq, E. *Curr. Opin. Pharmacol.* **2010**, *10*, 507–515.
- De Clercq, E. *J. Med. Chem.* **1995**, *38*, 2491–2517.
- Mely, Y.; Rocquigny, H. d.; Shvadchak, V.; Avilov, S.; Dong, C. Z.; Dietrich, U.; Darlix, J.-L. *Mini-Rev. Med. Chem.* **2008**, *8*, 24–35.
- Huang, M.; Maynard, A.; Turpin, J. A.; Graham, L.; Janini, G. M.; Covell, D. G.; Rice, W. G. *J. Med. Chem.* **1998**, *41*, 1371–1381.
- Lewis, M. G.; DaFonseca, S.; Chomont, N.; Palamara, A. T.; Tardugno, M.; Mai, A.; Collins, M.; Wagner, W. L.; Yalley-Ogunro, J.; Greenhouse, J.; Chirullo, B.; Norelli, S.; Garaci, E.; Savarino, A. *AIDS* **2011**, *25*, 1347–1356.
- Levin, J. G.; Guo, J.; Rouzina, I.; Musier-Forsyth, K. *Prog. Nucleic Acid Res. Mol. Biol.* **2005**, *80*, 217–286.